Different Interfacial Behaviors of Peptides Chemically Immobilized on Surfaces with Different Linker Lengths and via Different Termini

ARTICLE *in* THE JOURNAL OF PHYSICAL CHEMISTRY B · FEBRUARY 2014

Impact Factor: 3.3 · DOI: 10.1021/jp4122003 · Source: PubMed

THE JOURNAL OF PHYSICAL CHEMISTRY B

Article

pubs.acs.org/JPCB

Different Interfacial Behaviors of Peptides Chemically Immobilized on Surfaces with Different Linker Lengths and via Different Termini

Xiaofeng Han,[†,⊥] Yuwei Liu,[†] Fu-Gen Wu,[†,⊥] Joshua Jansensky,[‡] Taehoon Kim,[†] Zunliang Wang,[†,⊥] Charles L. Brooks, III,[†,‡] Jianfeng Wu,[§] Chuanwu Xi,[§] Charlene M. Mello,[∥] and Zhan Chen*[,†,‡]

[†]Department of Chemistry, [‡]Department of Biophysics, and [§]Department of Environmental Health Sciences, University of Michigan, Ann Arbor, Michigan 48109, United States

[∥]Bioscience and Technology Team, U.S. Army Natick Soldier Research, Development, & Engineering Center, 15 Kansas Street, Natick, Massachusetts 01760, United States

Supporting Information

ABSTRACT: Molecular structures such as conformation and orientation are crucial in determining the activity of peptides immobilized to solid supports. In this study, sum frequency generation (SFG) vibrational spectroscopy was applied to investigate such structures of peptides immobilized on self-assembled monolayers (SAMs). Here cysteine-modified antimicrobial peptide cecropin P1 (CP1) was chemically immobilized onto SAM with a maleimide terminal group. Two important characteristics, length of the poly(ethylene glycol) (PEG) segment in the SAM and location of the cysteine residue in the peptide, were examined using SFG spectroscopy to determine the effect of each on surface immobilization as well as peptide secondary structure and its orientation in the immobilized state. Results have shown that while each length of PEG chain studied promotes chemical immobilization of the target peptide and prevents nonspecific adsorption, CP1 immobilized on long-chain (PEG2k) maleimide SAMs shows random coil structure in water, whereas CP1 demonstrates α-helical structure when immobilized on short-chain (with four ethylene glycol units - (EG4)) maleimide SAMs. Placement of the cysteine residue at the C-terminus promotes the formation of α-helical structure of CP1 with a single orientation when tethered to EG4 maleimide SAM surfaces. In contrast, immobilization via the N-terminal cysteine of CP1 results in a random coil or lying-down helical structure. The bacteria capturing/killing capability was tested, showing that the surface-immobilized CP1 molecules via C- and N- terminal cysteine exhibit only slight difference, even though they have different secondary structures and orientations.

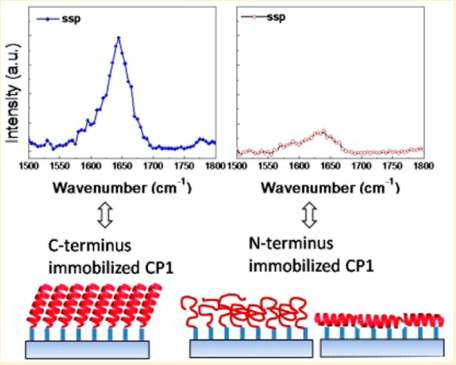

1. INTRODUCTION

Antimicrobial peptides (AMPs) serve as integral components to the immune system of many species of animals. The potency, broad range of activity, and affinity toward microorganisms render them potential candidates for novel therapeutic agents, adaptive antibiotics, and capture agents for bacteria after surface immobilization.[1−7] In addition, biological devices to access surfaces biological functions including cell signaling, cell adhesion, targeted immune responses, and catalytic reactions are rapidly emerging to include peptide-based receptors.[5−15] Immobilized peptides may also serve as linkers for the attachment and orientational control of enzymes or other proteins to solid supports.[16−19]

Because of the excellent selectivity and potency, AMP-based assays are beginning to outperform other common biosensing devices that are based on antibody−antigen binding and DNA amplification procedures such as polymerase chain reaction (PCR). For example, methods that use AMP-based assays have demonstrated to be easier than PCR and exhibit a broader range of bacterial targets over the antibody−antigen sensing techniques. Numerous bacterial biosensors based on AMPs have been developed.[7,8,19−23] A key component for a biosensor device is the biological recognition element, which interacts with the target pathogen. The performance of the biosensor (e.g., sensitivity, selectivity, detection limit, precision, accuracy, reproducibility, working life, and shelf life) is greatly dependent on the conformations and orientations of this biological recognition element, usually interfacial sensing biological molecules. In the case of peptide-based biomolecules, preservation of secondary structure and orientation are two of the most important criteria for high-quality sensor development.[24,25] Numerous surface peptide "anchoring" methods have been used to improve the performance of peptide-based biosensors, but the relationship between the peptide molecular structure (e.g., conformation and orientation) and the sensor performance has not yet been elucidated due to a lack of proper analytical techniques for surface protein and peptide characterization, especially in aqueous environments.

Received: December 13, 2013
Revised: February 17, 2014
Published: February 20, 2014

Many analytical techniques have been used for the characterization of surface immobilized peptides, including scanning tunneling microscopy,[26] electrical impedance spectroscopy,[27] X-ray photoelectron spectroscopy,[25,27] Fourier transform infrared (FTIR) spectroscopy, and circular dichroic (CD) spectroscopy.[27] These techniques have provided important information regarding basic understanding of peptide/protein structures and conformations; however, they either lack surface sensitivity or in situ capability, limiting their use in elucidating the surface peptide structures in situ. Recently, sum frequency generation (SFG) vibrational spectroscopy has been applied to investigate peptides and proteins at solid/liquid interfaces in situ.[28−44] SFG is a second-order nonlinear optical spectroscopic technique that has submonolayer surface specificity. In our group, we have successfully developed systematic methodologies to determine interfacial orientations of various secondary structures such as the α-helix, 3_{10} helix, β-sheet, and complex proteins such as heterotrimeric G proteins using polarized SFG spectra.[28−30,45] We applied these methods to deduce interfacial orientations of a variety of peptides and proteins including magainin 2, melittin, alamethicin, GRK2, and tachyplesin I.[28−31,45,46] In particular, we examined orientation of physically adsorbed and chemically immobilized α-helical cecropin P1 (CP1) on polymer surfaces.[32,47] To ensure chemical immobilization, the C-terminus of CP1 was modified with a cysteine residue (CP1c), which forms a stable thioether linkage with maleimide-derivatized polystyrene (PS-MA). Physical adsorption of CP1c onto a polystyrene surface yielded a multiple-orientation distribution and could not be described by a delta or Gaussian distribution.[47] However, CP1c peptides chemically immobilized onto the PS-MA exhibited an orientation angle of 35° versus the surface normal. When the cysteine was moved to the N-terminus of CP1(cCP1), cCP1 exhibited a single orientation distribution at the PS-MA/peptide solution interface at low peptide concentrations. At higher peptide concentrations ($\geq$1.23 μM), the cCP1 peptides adopted a multiple-orientation distribution.

In this work, we applied SFG spectroscopy to investigate molecular structure of immobilized peptides on maleimide-terminated self-assembled monolayers (SAMs). Our study described herein aims to characterize the extent of secondary structure and orientation of CP1 on maleimide SAMs with two different PEG lengths (PEG2k and EG4 − four ethylene glycol units) as well as two different attachment points on CP1 (cCP1 and CP1c). Lastly, the activity of immobilized CP1 was measured to characterize the relationship between immobilized peptide structure and bacteria capturing/killing ability.

2. EXPERIMENTAL SECTION

2.1. Substrates and Maleimide SAM Growth. Typically SAMs are prepared on gold, SiO_2, or Si surfaces. These materials are not transparent to infrared wavelengths, which are used to monitor the amide I group of CP1 (1500−1800 cm^{-1}). To have a substrate that was not only transparent in the infrared but also reactive to the silane end groups in our SAMs, we deposited a 100 nm layer of SiO_2 film onto a CaF_2 substrate. The schematic of substrate preparation and sample geometry is detailed in Figure 1. Right-angle CaF_2 prisms were purchased from Altos Photonics (Bozeman, MT). These CaF_2 prisms were soaked in toluene (purchased from Aldrich (Milwaukee, WI) and used as received) for 24 h and then sonicated in 1% Contrex AP solution from Decon Laboratories (King of Prussia, PA) for 10 min. The prisms were thoroughly rinsed with Millipore deionized water (18.2 MΩ cm) and dried under N_2. They were placed in an oxygen benchtop plasma cleaner (PE-25-JW) purchased from Plasma Etch (Carson City, NV) for 4 min immediately before being coated with SiO_2. A layer of 100 nm of SiO_2 was deposited onto the CaF_2 prisms by an electron-beam deposition process using a SJ-26 Evaporator system at a pressure below 10^{-5} Torr at a deposition rate of 5 Å/s.

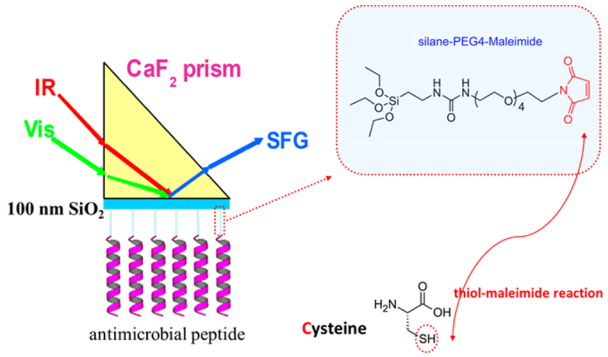

Figure 1. Schematic of CP1 molecules immobilized to a maleimide SAM on a CaF_2 prism substrate.

The SiO_2-coated CaF_2 prisms were treated with O_2 plasma for 4 min. O_2 plasma generates hydroxyl groups on SiO_2 surface, which react with the silane end groups of our SAMs. Once the prisms had been coated and cleaned, they were placed into a solution of 1 mM maleimide-EG4-silane (Mal-EG4, Creative PEGWorks, Winston Salem, NC, chemical structures are shown in Figure 1) or maleimide-PEG2k-silane (Mal-PEG2k, Nanocs, New York, NY) in anhydrous toluene for 48 h at room temperature. The only difference between Mal-EG4 and Mal-PEG2k is that the four ethylene glycol units in Mal-EG4 were replaced by a PEG segment with a molecular weight of 2k. Finally, the functionalized prisms were rinsed with copious amounts of toluene, followed by methanol and were dried with nitrogen. Anhydrous toluene and methanol were purchased from Aldrich (Milwaukee, WI) and used as received.

2.2. Cecropin P1 Immobilization. N-terminus cysteine modified cecropinP1 (cCP1, H_2N-CSWLSKTAKKLENSAKKRISEGIAIAIQGGPR−OH, M_W = 3442) and C-terminus modified cecropinP1 (CP1c, H_2N-SWLSKTAKKLENSAKKRISEGIAIAIQGGPRC−OH, M_W = 3442) were purchased from New England Peptide (Gardner, MA). Potassium phosphate (monobasic and dibasic) solution (PB) (1 M) and tris(2-carboxyethyl) phosphine hydrochloride (TCEP) solution (0.5 M) were purchased from Aldrich (Milwaukee, WI). Ethylenediaminetetraacetic acid (EDTA) was obtained from Fisher Biotech. The thiol moiety in the cysteine residue has a strong affinity for the maleimide moiety, which promotes the covalent immobilization of the peptide to the SAM-maleimide surface. EDTA and TCEP were added as a chelating and reducing agents, respectively, to oxidize any metals present in the buffer that may cause the formation of unwanted disulfide bonds as well as maintain the cysteine residues in a reduced state.

Peptide solutions of CP1 were prepared by dissolving 1.87 μM of either cCP1 or CP1c into 5 mM phosphate buffer with 0.03 mM TCEP and 0.01 mM EDTA. The resulting solution was placed in contact with the CaF_2 substrate and SAM surface. During the immobilization process, the SFG amide I signal was recorded, which indicates the immobilization of peptides to the

dx.doi.org/10.1021/jp4122003 | J. Phys. Chem. B 2014, 118, 2904−2912

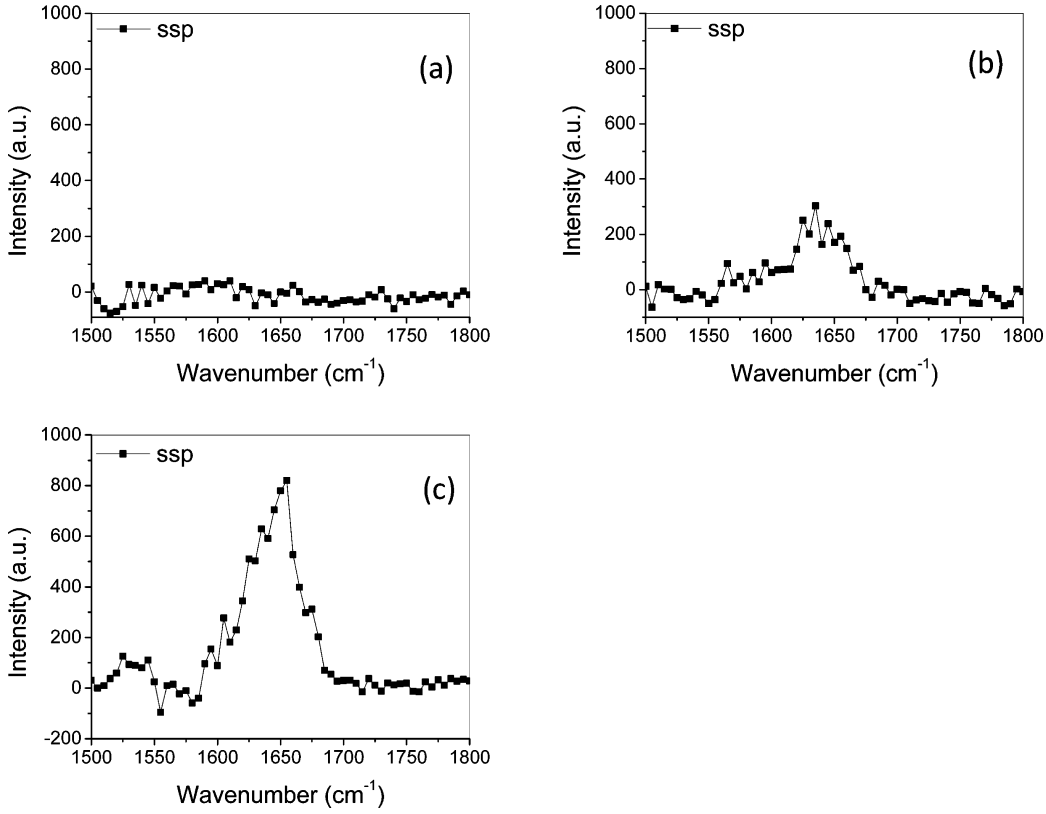

Figure 2. (a) SFG spectrum of the Mal-PEG2k SAM/PB solution interface. (b) SFG spectrum of the Mal-PEG2k SAM immobilized with CP1c in contact with a PB solution. (c) SFG spectrum of the Mal-PEG2k SAM immobilized with CP1c in contact with a TFE-PB 50%−50% mixture solution.

SAM surface. Once equilibrium was reached (~2 h after initial contact), SFG spectra of maleimide terminated SAM/CP1 PB solution were collected. Initially, the spectra can be contributed by both chemically immobilized and physically adsorbed peptides. To remove physically adsorbed peptides, the CP1 PB solution was replaced with pure PB. After three separate washes using the pure phosphate buffer solution, SFG spectra of chemically immobilized CP1 on maleimide SAMs were collected.

2.3. SFG Measurements. Details regarding SFG theories and equipment have been previously reported[48−53] and will not be repeated here. All of the SFG experiments were carried out at the room temperature (23 °C). SFG spectra with different polarization combinations including ssp (s-polarized SF output, s-polarized visible input, and p-polarized infrared input) and ppp were collected using the near total internal reflection geometry.[54]

2.4. Immobilized Peptide Antimicrobial Activity Test. SAM solutions with two different PEG lengths (Mal-PEG2k and Mal-EG4) were prepared using an identical procedure, as outlined in Section 2.1. Glass slides were presoaked in the SAM solutions to prepare maleimide-functionalized surfaces for peptide immobilization. These slides were then incubated in a 1.87 μM CP1 PB solution (pH 7.2, containing 30 μM TCEP and 10 μM EDTA) for 2 h to immobilize the cysteine-modified CP1 onto the maleimide SAMs. After washed by DI water, these slides were then placed into a Corning 15 mL tube with 2 mL of Luria−Bertani (LB) media. Overnight-grown *E. coli* was inoculated at a concentration of ~1 × 10^5 CFU/mL to each Corning tube, and tubes were placed in a 37.5 °C incubater with shaking at 150 rpm for 18 h.[55] After incubation, the slides were removed and rinsed with sterile 1× PBS buffer three times and then stained with appropriate concentration of fluorescent dyes, SYTO-9, and propidium iodide for 20 min in the dark according to the instructions for the LIVE/DEAD *BacLight* bacterial viability kit (L7012, Invitrogen, Carlsbad, CA). Stained slides were observed under a fluorescence microscope (Olympus 1 × 71, Center Valley, PA) equipped with a fluorescence illumination system (X-Cite 120, EXFO) and appropriate filter sets. Images were acquired using a 60× objective lens at five random spots on slides.

3. RESULTS AND DISCUSSION

Our previous work has shown that SFG is a powerful tool for structural analysis of immobilized or adsorbed peptides on surfaces.[32,56] Not only has SFG been demonstrated to have submonolayer sensitivity but also the amide I peak characteristic of peptides and proteins is very sensitive to the local environment, allowing for SFG to characterize the nature of secondary structure presented at the surface. Compared with attenuated total reflectance FTIR (ATR-FTIR), another common surface-sensitive technique, the SFG amide I peak (~1650 cm^{-1}) of α-helical structure seen in SFG, has minimal interference from the peak for random coil structures. Because of the selection rules that govern second-order nonlinear effects such as SFG, the random oriented groups in a random coil structure generate a much weaker SFG signal. Orientational analysis of surface peptides requires the collection of SFG spectra with different polarization combinations (e.g., ppp and ssp). For an α-helix, we have shown previously that the χ_{ppp}/χ_{ssp} signal strength ratio (taken after fitting the ppp and ssp spectra) can be used to determine its orientation.[30,32,37] The relationship

dx.doi.org/10.1021/jp4122003 | J. Phys. Chem. B 2014, 118, 2904−2912

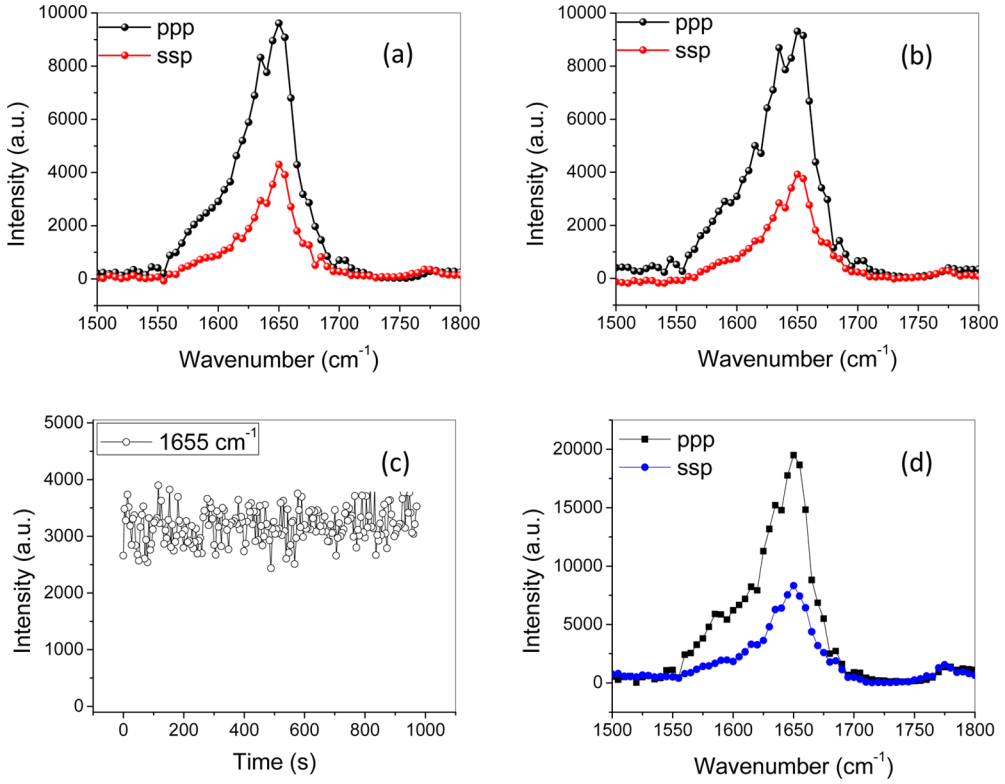

Figure 3. (a) SFG spectra of the Mal-EG4 SAM/CP1c PB solution interface. (b) SFG spectra of the Mal-EG4 SAM immobilized with CP1c in contact with a PB solution after PB buffer wash. (c) Time-dependent SFG signal (ssp) at 1650 cm^{-1} collected from the wash process after peptide immobilization. (d) SFG spectra of the Mal-EG4 SAM immobilized with CP1c in contact with a TFE-PB 50%−50% mixture solution (ppp and ssp).

between the χ_{ppp}/χ_{ssp} signal strength ratio and the CP1 orientation described by a delta or Gaussian distribution has been shown in our previous paper.[32]

In our previous work, we had studied CP1 immobilized on a polystyrene maleimide (PS-MA) polymer where it was shown that CP1c molecules at the PS-MA/CP1c buffer solution interface adopted a multiple-orientation distribution.[47] The χ_{ppp}/χ_{ssp} signal strength ratio was beyond the possible range described by a delta or Gaussian distribution that is indicative of both chemically immobilized and physically adsorbed species. Once the PS-MA surface was thrice washed with PB solution, the measured CP1c orientation could be described by a single orientation value. The following sections will present the experimental results obtained of the structures and orientations of CP1 immobilized on the PEG SAMs with maleimide end group. Results described herein will compare the structure and orientation of CP1 as sample parameters (including the length of PEG as well as the location of the cysteine residue within CP1) are varied.

3.1. Impact of PEG Length on Immobilized CP1c Structure. Previous studies that performed activity tests of immobilized AMPs have demonstrated that immobilized AMPs with a longer linker exhibit better antimicrobial activity.[57] Here we applied SFG to study the effect of different PEG lengths of the maleimide terminated SAM on the structure of immobilized CP1c. One long-chain PEG (PEG2k) and one short-chain EG4 were investigated. The SFG spectrum collected from the Mal-PEG2k SAM/PB solution interface is shown in Figure 2a. No discernible SFG signal can be detected in the amide I frequency region, showing that the maleimide groups are not present at the interface or are disordered at the interface. We then added the CP1c stock solution to the PB buffer in contact with the SAM to immobilize CP1c on the Mal-PEG2k SAM. SFG spectra were then collected from the SAM/CP1c PB solution interface(not shown) and also collected after replacing the peptide solution with PB solution several times (washing several times); identical SFG spectra were observed. As shown in Figure 2b, this time the SFG amide I signal can be detected but is very weak with the peak center at ∼1640 cm^{-1}.This indicates that the CP1c-immobilized peptides exhibit random -coil structure at the SAM/PB solution interface. The weak SFG signal may be because of the small amount of immobilized peptides, the randomly oriented peptides, or both.

The 2,2,2-trifluoethanol (TFE) is often used as a membrane mimic and is known for inducing a conformational transformation in peptides from random coil to α-helix.[58] With this information, we replaced the PB solution with 50%−50% TFE−PB mixture solution and then collected SFG spectra from the immobilized CP1 at the SAM/50%−50% TFE−PB mixture solution interface. Figure 2c shows the presence of an amide I peak of α-helical structure with the peak center at ∼1650 cm^{-1}. These results demonstrate that CP1 was successfully immobilized to the PEG2k SAM surface, although presenting a random coil structure. The addition of TFE to the PB solution was able to change the conformation of the attached peptides and recover a well-ordered α-helical structure.

The same procedures were repeated for the short PEG chain maleimide-terminated SAMs. It was our initial hypothesis that SAM molecules with short EG chain length should result in CP1 peptides with a more rigid molecular orientation than long PEG length due to the rigidity and compactness of the SAM surface. Short-chain PEG SAMs were composed of four ethylene glycol units within the PEG linker, in comparison with ∼45 units of PEG2k. SFG ssp and ppp spectra were

dx.doi.org/10.1021/jp4122003 | J. Phys. Chem. B 2014, 118, 2904−2912

collected from immobilized CP1c at the SAM/peptide PB solution interface and are shown in Figure 3a. The dominant peak in both ssp and ppp spectra is centered at 1650 cm^{-1},which is mainly contributed from an α-helical conformation. The SFG spectra can be fitted with two peaks: a weak peak at ~1610 cm^{-1} and a strong signal at 1650 cm^{-1}. The weak 1610 cm^{-1} peak is attributed to the CO signal of the maleimide group on the SAM surface. The signal strength ratio χ_{ppp}/χ_{ssp} can be calculated from the spectra fitting parameters of the amide I band in the ppp- and ssp-polarized SFG spectra. The deduced ratio from the chemically immobilized CP1c on EG4 maleimide SAM is 1.54, which corresponds to an orientation angle of ~35° versus the surface normal for the α-helical peptide assuming that the peptides exhibit a delta orientation distribution.

In contrast with the interactions between CP1c and the PS-MA surface, which lead to both chemical immobilization and physical adsorption,[47] here SAMs with four EG segments were able to prevent physical adsorption to the surface. Figure 3b presents the SFG ssp and ppp spectra collected from interfacial CP1c at the SAM/PB interface after the SAM surface (with CP1c) washed several times using PB solution. Both spectral features and the signal intensities are similar to those detected from CP1c at the SAM/CP1c solution without washing. This shows that the CP1c molecules at the interface are chemically immobilized. If physically adsorbed molecules exist at the interface, they would be washed off by PB solution, leading to reduced SFG signal intensity, which was not observed. Also, the measured signal strength ratio χ_{ppp}/χ_{ssp} from CP1c molecules at the SAM/CP1c PB solution interface leads to a delta orientation distribution, which is different from the CP1c at the PS-MA/CP1c PB solution interface. At the latter interface, the measured signal strength ratio χ_{ppp}/χ_{ssp} cannot satisfy a delta or Gaussian orientation distribution due to the presence of both chemically immobilized and physically adsorbed peptides. Here the delta orientation distribution shows that all peptides are chemically immobilized. To further demonstrate the absence of physically adsorbed peptide, Figure 3c shows a time dependent SFG signal (ssp) of 1650 cm^{-1} collected during the wash process after CP1c immobilization, indicating no decrease in the signal intensity. These results demonstrate that CP1c can be chemically immobilized on a maleimide SAM surface. The EG segments in SAMs effectively prevent the physical adsorption of peptides.

In testing the two maleimide-terminated SAMs with different lengths of PEG segments and their ability to immobilize CP1 peptide, it was observed that the EG4 SAM peptide immobilization produced not only a stronger amide I signal versus the PEG2k SAM peptide immobilization but also a more ordered conformation without the use of TFE. The reduced signal of CP1c on Mal-PEG2k SAM is thought to be caused by a lack of surface maleimide groups available to the CP1c for chemical immobilization. An apparent "lower" density of maleimide would result in a reduction in SFG signal, which was investigated through molecular dynamics (MD) simulations (shown in Figure 4). Figure 4 shows clearly that the surface density of the maleimide group of Mal-PEG 2k SAM is much lower than that of Mal-EG4 SAM.

3.2. Effect of Peptide Immobilization Site on CP1 Conformation. A number of studies have been performed to test antimicrobial activity[57,59] and lipopolysaccharides (LPS) binding ability of AMPs.[23] Uzarski and Mello found that the immobilized CP1 through the C-terminus tethered to SAM had much better LPS binding ability than peptides bound through the N-terminus. The CP1 peptide has hydrophobic C-terminus and amphiphilic N-terminus. Immobilization through CP1 C-terminus or N-terminus on surface may substantially affect the peptide structure. On the basis of this assumption, we decided to determine the conformation and orientation of CP1 through the immobilization of both the C- and N-termini. Parameters such as conformation and orientation may have a significant impact on both LPS binding and antimicrobial activity; therefore, it is crucial to understand and characterize their behavior.

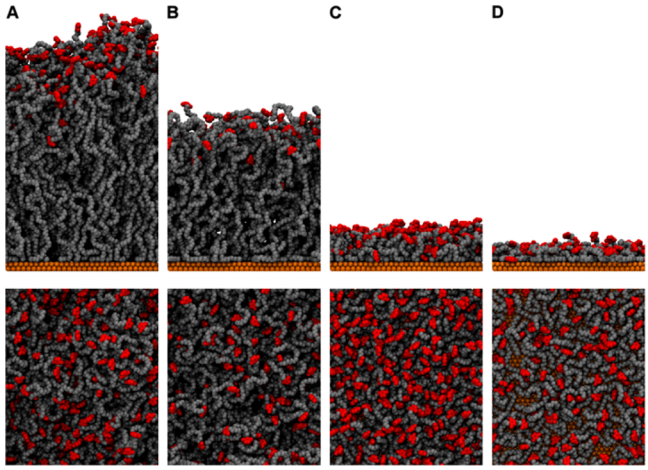

Figure 4. Side (top) and top (bottom) views of Mal-PEG 2k and Mal-EG4 SAM systems after production run of 20 ns. (A) $c(2 \times 1)$ and (B) $c(4 \times 2)$ unit cell of Mal-PEG2k. (C) $c(2 \times 1)$ and (D) $c(4 \times 2)$ unit cell of Mal-EG4: red, maleimide; gray, carbon, oxygen, and sulfur; orange, gold; bulk water is omitted for clarity. More details about the MD simulation can be found in the Supporting Information.

In the previous section, CP1c was chemically immobilized onto an EG4 SAM surface. Strong α-helical signal at 1650 cm^{-1} was present without the need for addition of TFE, and the signal strength ratio produced an orientation of ~35° versus the surface normal. Under the same conditions, cCP1 was immobilized onto Mal-EG4 SAMs. In contrast with C-terminus binding, the cCP1 at the Mal-EG4 SAM/cCP1 PB solution interface showed a very weak SFG peak in amide I range. Figure 5a displays the SFG spectra of cCP1 at Mal-EG4 SAMs/cCP1 PB solution interface (open dot). The solid dots show the SFG spectra of pure Mal-EG4 SAM contacting with PB solution before adding cCP1. Again, the peak with center 1625 cm^{-1} is due to the maleimide group. Therefore, there is minimal difference in the observed SFG spectra upon cCP1 immobilization.

No detected SFG signals from the SAM/cCP1 solution interface may be due to no peptide binding to the maleimide-terminated SAM surface, a random coil structure of the peptide bound, or an α-helical structure lying down. The SAM surface was thrice washed then contacted with TFE-PB 50%−50% mixture solution, as done for the CP1c immobilization on the Mal-PEG2k SAM. The amide I signal increased dramatically with its peak center at 1650 cm^{-1}, as shown in Figure 5b. This result indicates that the cCP1 did immobilize on Mal-EG4 SAMs however was in a random-coil structure or a lying-down helical structure and required TFE to induce α-helical formation or orientational change. Figure 5c shows the ppp and ssp spectra detected from immobilized cCP1 at the Mal-EG4 SAM/TFE-PB 50%−50% solution interface. According to

dx.doi.org/10.1021/jp4122003 | J. Phys. Chem. B 2014, 118, 2904−2912

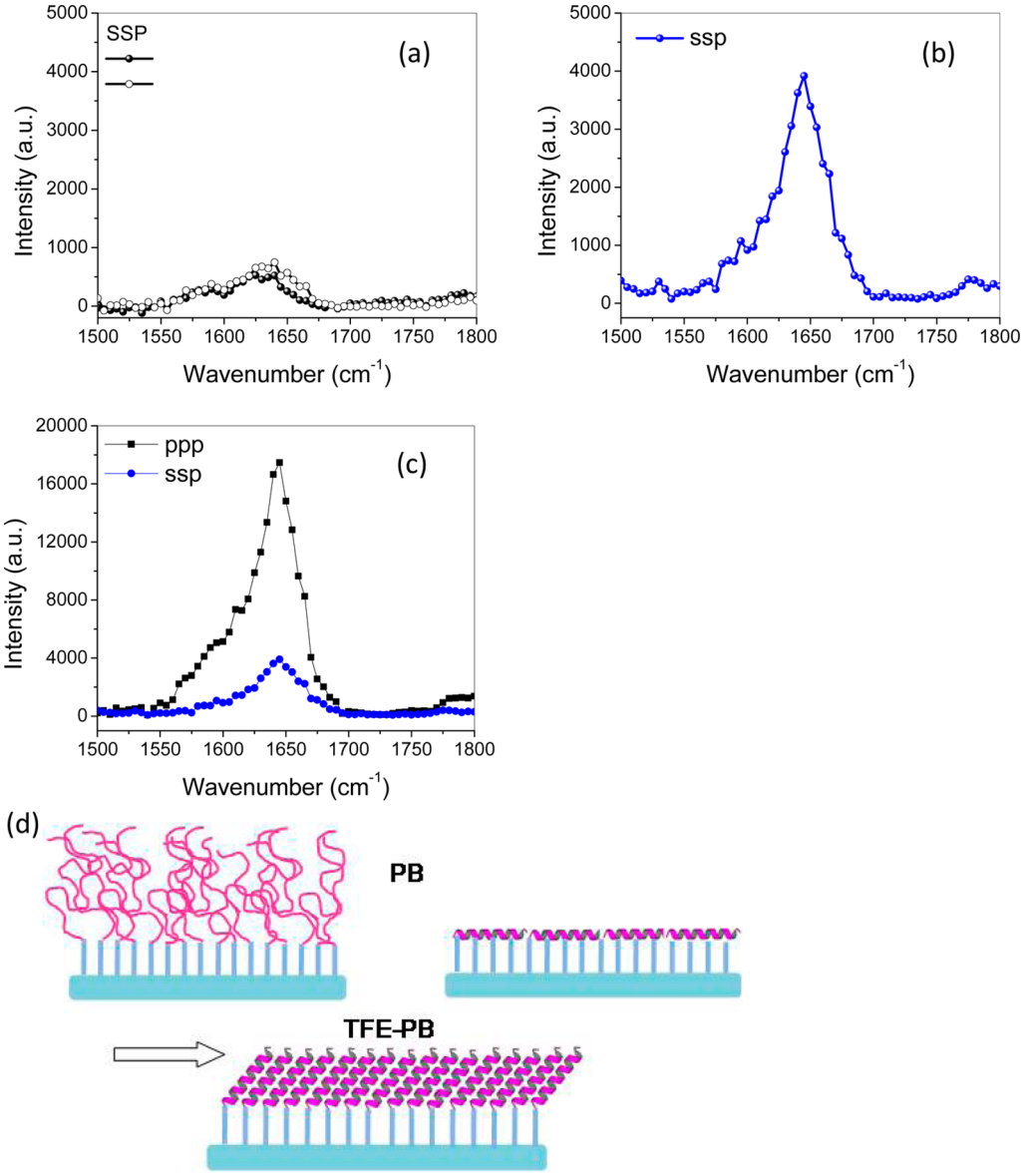

Figure 5. (a) SFG spectra of the Mal-EG4 SAMs/PB solution interface (solid circle) and the Mal-EG4 SAM/cCP1 PB solution interface (open circle) (b) SFG spectrum of Mal-EG4 SAM immobilized with cCP1 in contact with a PB solution after PB wash. (c) SFG spectra of Mal-EG4 SAM immobilized with cCP1 in contact with a TFE-PB 50%−50% mixture solution (ppp and ssp). (d) Schematic of cCP1 conformation change at different interface condition: contacting with PB or TFE-PB solution.

the spectral fitting results, the SFG signal strength ratio χ_{ppp}/χ_{ssp} is 1.94. Under this condition, the immobilized peptides have a single orientational distribution with the orientation angle of 67°. A schematic representing the cCP1 conformation change under different interface conditions (contacting with PB or TFE-PB mixture solution) is shown in Figure 5d. The N-terminus, having six charged residues, may have a strong interaction with the ethylene glycol groups, preventing the peptide from forming an α-helical structure. After cCP1 immobilization, the C-terminus, having hydrophobic residues, cannot favorably interact with water molecules and may induce the peptide to lie down on the surface. The different conformations/orientations of immobilized cCP1 and CP1c can be elucidated in more detail using MD simulations, which will be published in the near future.

3.3. Antimicrobial Properties of Immobilized CP1 on SAMs. The SFG results demonstrate that different PEG linker lengths and different binding sites greatly affect the surface immobilized CP1 secondary structure and orientation. Solution-based antimicrobial tests were used here to investigate the relationship between immobilized peptide structure and the antimicrobial activity. Three kinds of CP1-immobilized surfaces (which were previously studied by SFG) were tested: Mal-PEG2k SAM immobilized with CP1c, Mal-EG4 SAM immobilized with CP1c, and Mal-EG4 SAM immobilized with cCP1. The antimicrobial activity testing procedure has been previously described in Section 2.4. The glass slides with SAMs immobilized with CP1 were soaked in 10^5 CFU/mL *E. coli* containing culturing solution for 18 h at 37.5 °C. Because the peptides were chemically immobilized on the surface of the test slides, no leaching of peptides into the solution is expected. No obvious inhibition on *E. coli* growth in the bacterial culture solution was observed.

dx.doi.org/10.1021/jp4122003 | J. Phys. Chem. B 2014, 118, 2904−2912

We observed that the slide surfaces were attached with bacteria cells stained with the Bacterial LIVE/DEAD dyes by fluorescence microscopy. We observed the surface-attached bacteria on slides by fluorescence microscopy after bacterial cells were stained with Bacterial LIVE/DEAD staining dyes. Figure 6 displays fluorescence images showing bacteria on

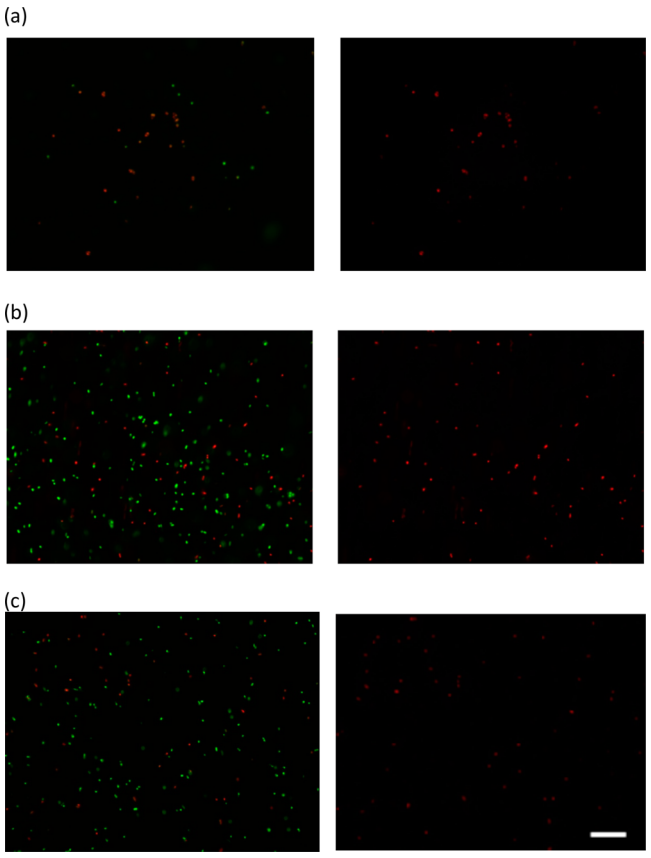

Figure 6. Representative fluorescence micrographs showing comparison of surfaces of Mal-PEG2k immobilized with CP1c (a), Mal-EG4 immobilized with CP1c (b), and Mal-EG4 immobilized with cCP1 (c) after soaking in 10^5 CFU/mL *E. coli* containing 50 mM GSH for 18 h at 37.5 °C. Bacterial cells were stained with Bacterial LIVE/DEAD staining dyes, and viable cells shown green while dead or membrane damaged cells shown red fluorescence in the images. Images shown in the left column contain a composite image of both alive and dead cells, whereas the right image contains only the dead cells from the corresponding cells on the left. Scale bar represents 20 μm in length and applies to all images.

different surfaces of Mal-PEG2k SAM immobilized with CP1c (a), Mal-EG4 SAM immobilized with CP1c (b), and Mal-EG4 SAM immobilized with cCP1 (c). In these graphs, viable cells generate green, while dead or membrane-damaged cells generate red fluorescence signals. Composite figures of both alive and dead cells are shown in the left panels, whereas the right panels show only the dead cells from the corresponding image on the left. From these images, the Mal-PEG2k surface with CP1c immobilized has much less attached and killed bacteria compared with those on the Mal-EG4 surface-immobilized with CP1c. This is consistent with our SFG results, which show that many fewer CP1c peptides are immobilized on the Mal-PEG2k surface due to lower quantities of maleimide groups available for immobilization (confirmed by the MD simulations). However, most of the bacteria adsorbed on the Mal-PEG2k surface were killed. For surfaces of CP1c and cCP1 immobilized on Mal-EG4, both surfaces have much more attached and killed bacteria compared with the Mal-PEG2k surface, but the ratio of the killed versus attached bacteria was less than that on the Mal-PEG2k surface. There was not a substantial difference in the numbers of attached or killed bacteria for either of the cecropin attachment sites on Mal-EG4; CP1c immobilization with an α-helical structure shows slightly better bacterial capturing/killing capability. If we assume that the CP1 peptides need to form (a standing-up) α-helical structure in the bacterial cell membrane to capture and kill bacteria, the observation demonstrates that the immobilized peptides originally with a random-coil structure or lying-down helical structure will change into α-helical structure or change its orientation in the bacterial cell membrane to capture and kill the bacteria. The TFE contacting SFG experiments of cCP1 (shown in Figure 5c) demonstrated this possibility: immobilized cCP1 adopts a tilted α-helical structure.

4. CONCLUSIONS

In this research, CP1 immobilization on SAM surfaces has been investigated in situ by using SFG spectroscopy. We studied the effects of different PEG lengths of maleimide SAMs on immobilized CP1c secondary structure. CP1c on long PEG SAMs shows random-coil structure, while the shorter PEG length exhibited α-helical conformation. The CP1c binding to Mal-EG4 also shows a single distribution with an orientation angle of 35° versus surface normal. In contrast, the immobilized CP1 bound to Mal-EG4 SAMs through its N-terminus showed random-coil structure or lying-down helical structure. From these results, we have demonstrated that the differences in the properties of the SAM and peptide binding site greatly affect the conformation and orientation of immobilized peptides. Such knowledge may be used to design tailored surfaces with proper conformation and orientation to maximize the surface efficiency and activity. More details of the different interactions between the CP1 with a cysteine group on different termini (e.g., cCP1 and CP1c) and Mal-EG4 SAM surface are being investigated using MD simulation, which will be reported in the future.

■ ASSOCIATED CONTENT

Ⓢ Supporting Information

Details of molecular dynamics simulations on Mal-PEG2k SAM and Mal-EG4 SAM. This material is available free of charge via the Internet at http://pubs.acs.org.

■ AUTHOR INFORMATION

Corresponding Author

*Phone: (734) 615-4189. E-mail: zhanc@umich.edu.

Present Address

⊥X.H., F.W., and Z.W.:
School of Biological Science and Medical Engineering, Southeast University, Nanjing, China, 210096.

Notes

The authors declare no competing financial interest.

■ ACKNOWLEDGMENTS

This work is supported by Army Research Office (W911NF-11-1-0251), Defense Threat Reduction Agency (HDTRA1-11-1-0019), U.S. Army Natick Research, Development and Engineering Center (W911QY-10-C-0001), the National

Natural Science Foundation of China (Grant: 21303015), and the Priority Academic Program Development of Jiangsu Higher Education Institutions (1107037001). We also like to thank the Lurie Nanofabrication Facility for their resources.

REFERENCES

(1) Gregory, K.; Mello, C. M. Immobilization of Escherichia coli cells by use of the antimicrobial peptide cecropin P1. *Appl. Environ. Microbiol.* **2005**, *71* (3), 1130−1134.
(2) Arcidiacono, S.; Pivarnik, P.; Meehan, A.; Mello, C.; Senecal, A. *Labeled Antimicrobial Peptides for Detection of Microorganisms*; DTIC Document; Defense Technical Information Center: Fort Belvoir, VA, 2008.
(3) Mello, C. M.; Soares, J. Membrane Selectivity of Antimicrobial Peptides. *ACS Symp. Ser.* **2008**, *984*, 51−62.
(4) Soares, J. W.; Kirby, R.; Morin, K. M.; Mello, C. M. Antimicrobial peptide preferential binding of E. Coli o157: H7. *Protein Pept. Lett.* **2008**, *15* (10), 1086−1093.
(5) Kulagina, N. V.; Shaffer, K. M.; Anderson, G. P.; Ligler, F. S.; Taitt, C. R. Antimicrobial peptide-based array for *Escherichia coli* and *Salmonella* screening. *Anal. Chim. Acta* **2006**, *575* (1), 9−15.
(6) Shriver-Lake, L. C.; North, S. H.; Dean, S. N.; Taitt, C. R. Antimicrobial Peptides for Detection and Diagnostic Assays. In *Designing Receptors for the Next Generation of Biosensors*; Piletsky, S. A., Whitcombe, M. J., Eds.; Springer: New York, 2013; Vol. *12*, pp 85−104.
(7) Kulagina, N. V.; Lassman, M. E.; Ligler, F. S.; Taitt, C. R. Antimicrobial peptides for detection of bacteria in biosensor assays. *Anal. Chem.* **2005**, *77* (19), 6504−6508.
(8) Mannoor, M. S.; Zhang, S.; Link, A. J.; McAlpine, M. C. Electrical detection of pathogenic bacteria via immobilized antimicrobial peptides. *Proc. Natl. Acad. Sci.* **2000**, *107* (45), 19207−19212.
(9) Ulevitch, R. J. Therapeutics targeting the innate immune system. *Nat. Rev. Immunol.* **2004**, *4* (7), 512−520.
(10) North, S. H.; Wojciechowski, J.; Chu, V.; Taitt, C. R. Surface immobilization chemistry influences peptide-based detection of lipopolysaccharide and lipoteichoic acid. *J. Pept. Sci.* **2012**, *18* (6), 366−372.
(11) Nakayama, H.; Manaka, T.; Iwamoto, M.; Kimura, S. Vertical orientation with a narrow distribution of helical peptides immobilized on a quartz substrate by stereocomplex formation. *Soft Matter* **2012**, *8* (12), 3387.
(12) Johnson, S.; Evans, D.; Laurenson, S.; Paul, D.; Davies, A. G.; Ferrigno, P. K.; Wälti, C. Surface-immobilized peptide aptamers as probe molecules for protein detection. *Anal. Chem.* **2008**, *80* (4), 978−983.
(13) Houseman, B. T.; Huh, J. H.; Kron, S. J.; Mrksich, M. Peptide chips for the quantitative evaluation of protein kinase activity. *Nat. Biotechnol.* **2002**, *20* (3), 270−274.
(14) Zaytseva, N. V.; Goral, V. N.; Montagna, R. A.; Baeumner, A. J. Development of a microfluidic biosensor module for pathogen detection. *Lab Chip* **2005**, *5* (8), 805−811.
(15) Lesaicherre, M. L.; Uttamchandani, M.; Chen, G. Y. J.; Yao, S. Q. Developing site-specific immobilization strategies of peptides in a microarray. *Bioorg. Med. Chem. Lett.* **2002**, *12* (16), 2079−2083.
(16) Jonkheijm, P.; Weinrich, D.; Schröder, H.; Niemeyer, C. M.; Waldmann, H. Chemical strategies for generating protein biochips. *Angew. Chem., Int. Ed.* **2008**, *47* (50), 9618−9647.
(17) Naffin, J. L.; Han, Y.; Olivos, H. J.; Reddy, M. M.; Sun, T.; Kodadek, T. Immobilized peptides as high-affinity capture agents for self-associating proteins. *Chem. Biol.* **2003**, *10* (3), 251−259.
(18) Fu, J.; Reinhold, J.; Woodbury, N. W. Peptide-modified surfaces for enzyme immobilization. *PLoS One* **2011**, *6* (4), e18692.
(19) Leonard, P.; Hearty, S.; Brennan, J.; Dunne, L.; Quinn, J.; Chakraborty, T.; O' Kennedy, R. Advances in biosensors for detection of pathogens in food and water. *Enzyme Microb. Technol.* **2003**, *32* (1), 3−13.
(20) Kato, R.; Kaga, C.; Kunimatsu, M.; Kobayashi, T.; Honda, H. Peptide array-based interaction assay of solid-bound peptides and anchorage-dependant cells and its effectiveness in cell-adhesive peptide design. *J. Biosci. Bioeng.* **2006**, *101* (6), 485−495.
(21) Strauss, J.; Kadilak, A.; Cronin, C.; Mello, C. M.; Camesano, T. A. Binding, inactivation, and adhesion forces between antimicrobial peptide cecropin P1 and pathogenic *E. coli*. *Colloids Surf., B* **2010**, *75* (1), 156−164.
(22) Ivnitski, D.; Abdel-Hamid, I.; Atanasov, P.; Wilkins, E. Biosensors for detection of pathogenic bacteria. *Biosens. Bioelectron.* **1999**, *14* (7), 599−624.
(23) Uzarski, J. R.; Mello, C. M. Detection and classification of related lipopolysaccharides via a small array of immobilized antimicrobial peptides. *Anal. Chem.* **2012**, *84*, 7359−7366.
(24) Ivanov, I. E.; Morrison, A. E.; Cobb, J. E.; Fahey, C. A.; Camesano, T. A. Creating Antibacterial Surfaces with the Peptide Chrysophsin-1. *ACS Appl. Mater. Interfaces* **2012**, *4*, 5891−5897.
(25) Nowinski, A. K.; Sun, F.; White, A. D.; Keefe, A. J.; Jiang, S. Sequence, structure, and function of peptide self-assembled monolayers. *J. Am. Chem. Soc.* **2012**, *134* (13), 6000−6005.
(26) Raigoza, A. F.; Webb, L. J. Molecularly Resolved Images of Peptide-Functionalized Gold Surfaces by Scanning Tunneling Microscopy. *J. Am. Chem. Soc.* **2012**, *134* (47), 19354−19357.
(27) Shamsi, F.; Coster, H.; Jolliffe, K. A.; Chilcott, T. Characterization of the substructure and properties of immobilized peptides on silicon surface. *Mater. Chem. Phys.* **2010**, *126* (3), 955−961.
(28) Chen, X.; Wang, J.; Boughton, A. P.; Kristalyn, C. B.; Chen, Z. Multiple orientation of melittin inside a single lipid bilayer determined by combined vibrational spectroscopic studies. *J. Am. Chem. Soc.* **2007**, *129* (5), 1420−1427.
(29) Nguyen, K. T.; King, J. T.; Chen, Z. Orientation determination of interfacial β-sheet structures in situ. *J. Phys. Chem. B* **2010**, *114* (25), 8291−8300.
(30) Nguyen, K. T.; Le Clair, S. V.; Ye, S.; Chen, Z. Orientation Determination of Protein Helical Secondary Structures Using Linear and Nonlinear Vibrational Spectroscopy. *J. Phys. Chem. B* **2009**, *113* (36), 12169−12180.
(31) Boughton, A. P.; Andricioaei, I.; Chen, Z. Surface orientation of magainin 2: Molecular dynamics simulation and sum frequency generation vibrational spectroscopic studies. *Langmuir* **2010**, *26* (20), 16031.
(32) Han, X.; Soblosky, L.; Slutsky, M.; Mello, C. M.; Chen, Z. Solvent Effect and Time-Dependent Behavior of C-Terminus-Cysteine-Modified Cecropin P1 Chemically Immobilized on a Polymer Surface. *Langmuir* **2011**, *27* (11), 7042−7051.
(33) Nguyen, K. T.; Soong, R.; lm, S. C.; Waskell, L.; Ramamoorthy, A.; Chen, Z. Probing the spontaneous membrane insertion of a tail-anchored membrane protein by sum frequency generation spectroscopy. *J. Am. Chem. Soc.* **2010**, *132* (43), 15112−15115.
(34) Okur, H. I.; Kherb, J.; Cremer, P. S. Cations Bind Only Weakly to Amides in Aqueous Solutions. *J. Am. Chem. Soc.* **2013**, *135* (13), 5062−5067.
(35) Huang, D.; Robison, A. D.; Liu, Y. Q.; Cremer, P. S. Monitoring protein-small molecule interactions by local pH modulation. *Biosens. Bioelectron.* **2012**, *38* (1), 74−78.
(36) Fu, L.; Liu, J.; Yan, E. C. Y. Chiral Sum Frequency Generation Spectroscopy for Characterizing Protein Secondary Structures at Interfaces. *J. Am. Chem. Soc.* **2011**, *133* (21), 8094−8097.
(37) Fu, L.; Ma, G.; Yan, E. C. Y. In Situ Misfolding of Human Islet Amyloid Polypeptide at Interfaces Probed by Vibrational Sum Frequency Generation. *J. Am. Chem. Soc.* **2010**, *132* (15), 5405−5412.
(38) Weidner, T.; Breen, N. F.; Li, K.; Drobny, G. P.; Castner, D. G. Sum frequency generation and solid-state NMR study of the structure, orientation, and dynamics of polystyrene-adsorbed peptides. *Proc. Natl. Acad. Sci. U.S.A.* **2010**, *107* (30), 13288−13293.
(39) Weidnerw, T.; Castner, D. G. SFG analysis of surface bound proteins: a route towards structure determination. *Phys. Chem. Chem. Phys.* **2013**, *15* (30), 12516−12524.

(40) Kim, J.; Somorjai, G. A. Molecular packing of lysozyme, fibrinogen, and bovine serum albumin on hydrophilic and hydrophobic surfaces studied by infrared-visible sum frequency generation and fluorescence microscopy. *J. Am. Chem. Soc.* **2003**, *125* (10), 3150−3158.
(41) Onorato, R. M.; Yoon, A. P.; Lin, J. T.; Somorjai, G. A. Adsorption of Amino Acids and Dipeptides to the Hydrophobic Polystyrene Interface Studied by SFG and QCM: The Special Case of Phenylalanine. *J. Phys. Chem. C* **2012**, *116* (18), 9947−9954.
(42) Wei, F.; Ye, S.; Li, H.; Luo, Y. Phosphate Ions Promoting Association between Peptide and Modeling Cell Membrane Revealed by Sum Frequency Generation Vibrational Spectroscopy. *J. Phys. Chem. C* **2013**, *117* (21), 11095−11103.
(43) Etayash, H.; Norman, L.; Thundat, T.; Kaur, K. Peptide-bacteria interactions using engineered surface-immobilized peptides from class IIa bacteriocins. *Langmuir* **2013**, *29* (12), 4048−4056.
(44) Roy, S.; Hung, K. K.; Stege, U.; Hore, D. K. Rotations, Projections, Direction Cosines, and Vibrational Spectra. *Appl. Spectrosc. Rev.* **2014**, *49* (3), 233−248.
(45) Boughton, A. P.; Yang, P.; Tesmer, V. M.; Ding, B.; Tesmer, J. J. G.; Chen, Z. Heterotrimeric G protein $\beta 1\gamma 2$ subunits change orientation upon complex formation with G protein-coupled receptor kinase 2 (GRK2) on a model membrane. *Proc. Natl. Acad. Sci. U.S.A.* **2012**, *108* (37), E667−E673.
(46) Ye, S.; Li, H.; Wei, F.; Jasensky, J.; Boughton, A. P.; Yang, P.; Chen, Z. Observing a Model Ion Channel Gating Action in Model Cell Membranes in Real Time in Situ: Membrane Potential Change Induced Alamethicin Orientation Change. *J. Am. Chem. Soc.* **2012**, *134* (14), 6237−6243.
(47) Ye, S.; Nguyen, K. T.; Boughton, A. P.; Mello, C. M.; Chen, Z. Orientation difference of chemically immobilized and physically adsorbed biological molecules on polymers detected at the solid/liquid interfaces in situ. *Langmuir* **2009**, *26* (9), 6471−6477.
(48) Belkin, M. A.; Shen, Y. R. Non-linear optical spectroscopy as a novel probe for molecular chirality. *Int. Rev. Phys. Chem.* **2005**, *24* (2), 257−299.
(49) Shen, Y. R. *The Principles of Nonlinear Optics*; Wiley-Interscience: New York, 1984, p 479−504.
(50) Shen, Y. R. Surface properties probed by second-harmonic and sum-frequency generation. *Nature* **1989**, *337*, 519−525.
(51) Williams, C. T.; Beattie, D. A. Probing buried interfaces with non-linear optical spectroscopy. *Surf. Sci.* **2002**, *500* (1), 545−576.
(52) Zhuang, X.; Miranda, P. B.; Kim, D.; Shen, Y. R. Mapping molecular orientation and conformation at interfaces by surface nonlinear optics. *Phys. Rev. B* **1999**, *59* (19), 12632.
(53) Lambert, A. G.; Davies, P. B.; Neivandt, D. J. Implementing the theory of sum frequency generation vibrational spectroscopy: A tutorial review. *Appl. Spectrosc. Rev.* **2005**, *40* (2), 103−145.
(54) Wang, J.; Mark, A.; Chen, X.; Schmaier, A. H.; Waite, J. H.; Chen, Z. Detection of amide I signals of interfacial proteins in situ using SFG. *J. Am. Chem. Soc.* **2003**, *125* (33), 9914−9915.
(55) Cai, W.; Wu, J.; Xi, C.; Ashe Iii, A. J.; Meyerhoff, M. E. Carboxyl-ebselen-based layer-by-layer films as potential antithrombotic and antimicrobial coatings. *Biomaterials* **2011**, *32* (31), 7774−7784.
(56) Ye, S.; Nguyen, K. T.; Clair, S. V. L; Chen, Z. In situ molecular level studies on membrane related peptides and proteins in real time using sum frequency generation vibrational spectroscopy. *J. Struct. Biol.* **2009**, *168* (1), 61−77.
(57) Bagheri, M.; Beyermann, M.; Dathe, M. Immobilization reduces the activity of surface-bound cationic antimicrobial peptides with no influence upon the activity spectrum. *Antimicrob. Agents Chemother.* **2009**, *53* (3), 1132−1141.
(58) Uzarski, J. R.; Tannous, A.; Morris, J. R.; Mello, C. M. The effects of solution structure on the surface conformation and orientation of a cysteine-terminated antimicrobial peptide cecropin P1. *Colloids Surf., B* **2008**, *67* (2), 157−165.
(59) Bagheri, M.; Beyermann, M.; Dathe, M. Mode of Action of Cationic Antimicrobial Peptides Defines the Tethering Position and the Efficacy of Biocidal Surfaces. *Bioconjugate Chem.* **2011**, *23* (1), 66−74.